J|A|C|S
ARTICLES

Published on Web 01/28/2009

Cleavage of Four Carbon−Carbon Bonds during Biosynthesis of the Griseorhodin A Spiroketal Pharmacophore

Zeynep Yunt,[†] Kathrin Reinhardt,[†] Aiying Li,[‡,#] Marianne Engeser,[†] Hans-Martin Dahse,[§] Michael Gütschow,[||] Torsten Bruhn,[⊥] Gerhard Bringmann,[⊥] and Jörn Piel*,[†]

Kekulé Institute of Organic Chemistry and Biochemistry and the Pharmaceutical Institute, University of Bonn, 53121 Bonn, Germany, Department of Bioorganic Chemistry, Max Planck Institute for Chemical Ecology, 07745 Jena, Germany, Department of Infection Biology Germany, Leibniz Institute for Natural Product Research and Infection Biology − Hans Knöll Institute, 07745 Jena, Germany, and Institute of Organic Chemistry, University of Würzburg, 97074 Würzburg, Germany

Received October 14, 2008; E-mail: joern-piel@uni-bonn.de

Abstract: The rubromycins, such as γ-rubromycin, heliquinomycin, and griseorhodin A, are a family of extensively modified aromatic polyketides that inhibit HIV reverse transcriptase and human telomerase. Telomerase inhibition crucially depends on the presence of a spiroketal moiety that is unique among aromatic polyketides. Biosynthetic incorporation of this pharmacophore into the rubromycins results in a dramatic distortion of the overall polyketide structure, but how this process is achieved by the cell has been obscure. To identify the enzymes involved in spiroketal construction, we generated 14 gene-deletion variants of the griseorhodin A biosynthetic gene cluster isolated from the tunicate-associated bacterium *Streptomyces* sp. JP95. Heterologous expression and metabolic analysis allowed for an assignment of most genes to various stages of griseorhodin tailoring and pharmacophore generation. The isolation of the novel advanced intermediate lenticulone, which exhibits cytotoxic, antibacterial, and elastase-inhibiting activity, provided direct evidence that the spiroketal is formed by cleavage of four carbon−carbon bonds in a pentangular polyketide precursor. This remarkable transformation is followed by an epoxidation catalyzed by an unusual cytochrome P450/NADPH:ubiquinone oxidoreductase pair that utilizes a saturated substrate. In addition, the absolute configuration of griseorhodin A was determined by quantum-chemical circular dichroism (CD) calculations in combination with experimental CD measurements.

Introduction

Natural products of the rubromycin group (Figure 1) are extensively modified aromatic polyketides isolated from a range of actinomycetes.[1−3] Their unique feature is a spiroketal moiety that interrupts the polyaromatic structure and causes it to adopt a distorted, nonplanar shape. Several members have been found to inhibit enzymes with reverse transcriptase activity, such as HIV reverse transcriptase[4] and human telomerase,[5] a promising target for cancer therapy.[6,7] Antitelomerase assays using compounds with intact spiroacetal units (e.g., **1**−**3**) and opened ones (i.e., **5**) revealed that the spiro system is crucial for high activity.[5] The identification of this pharmacophore now allows the exploration of possible ways that rubromycin analogues with improved pharmacological profiles may be generated. In particular, the low solubility in most solvents is an undesirable property of almost all natural rubromycins that could be eliminated by modification of the molecular periphery. Engineered biosynthesis, i.e., the genetic modification of metabolic routes, is one possible strategy for obtaining such novel compounds.[8] In order to identify the enzymes involved in pharmacophore generation, we have isolated the gene cluster (*grh* cluster) encoding the production of griseorhodin A (**1**), a highly oxygenated rubromycin analogue carrying an ep-

[†] Kekulé Institute of Organic Chemistry and Biochemistry, University of Bonn
[‡] Max Planck Institute for Chemical Ecology
[§] Leibniz Institute for Natural Product Research and Infection Biology
[||] Pharmaceutical Institute, University of Bonn
[⊥] University of Würzburg
[#] Present address: The College of Life Sciences, Central China Normal University, Wuhan 430079, China.

(1) Brasholz, M.; Sorgel, S.; Azap, C.; Reissig, H. U. *Eur. J. Org. Chem.* **2007**, 3801–3814.
(2) Puder, C.; Loya, S.; Hizi, A.; Zeeck, A. *Eur. J. Org. Chem.* **2000**, 729–735.
(3) Chino, M.; Nishikawa, K.; Tsuchida, T.; Sawa, R.; Nakamura, H.; Nakamura, K. T.; Muraoka, Y.; Ikeda, D.; Naganawa, H.; Sawa, T.; Takeuchi, T. *J. Antibiot.* **1997**, *50*, 143–146.
(4) Goldman, M. E.; Salituro, G. S.; Bowen, J. A.; Williamson, J. M.; Zink, D. L.; Schleif, W. A.; Emini, E. A. *Mol. Pharmacol.* **1990**, *38*, 20–25.
(5) Ueno, T.; Takahashi, H.; Oda, M.; Mizunuma, M.; Yokoyama, A.; Goto, Y.; Mizushina, Y.; Sakaguchi, K.; Hayashi, H. *Biochemistry* **2000**, *39*, 5995–6002.
(6) Chumsri, S.; Burger, A. M. *Curr. Opin. Mol. Ther.* **2008**, *10*, 323–333.
(7) Rezler, E. M.; Bearss, D. J.; Hurley, L. H. *Annu. Rev. Pharmacol. Toxicol.* **2003**, *43*, 359–379.
(8) Rix, U.; Fischer, C.; Remsing, L. L.; Rohr, J. *Nat. Prod. Rep.* **2002**, *19*, 542–580.

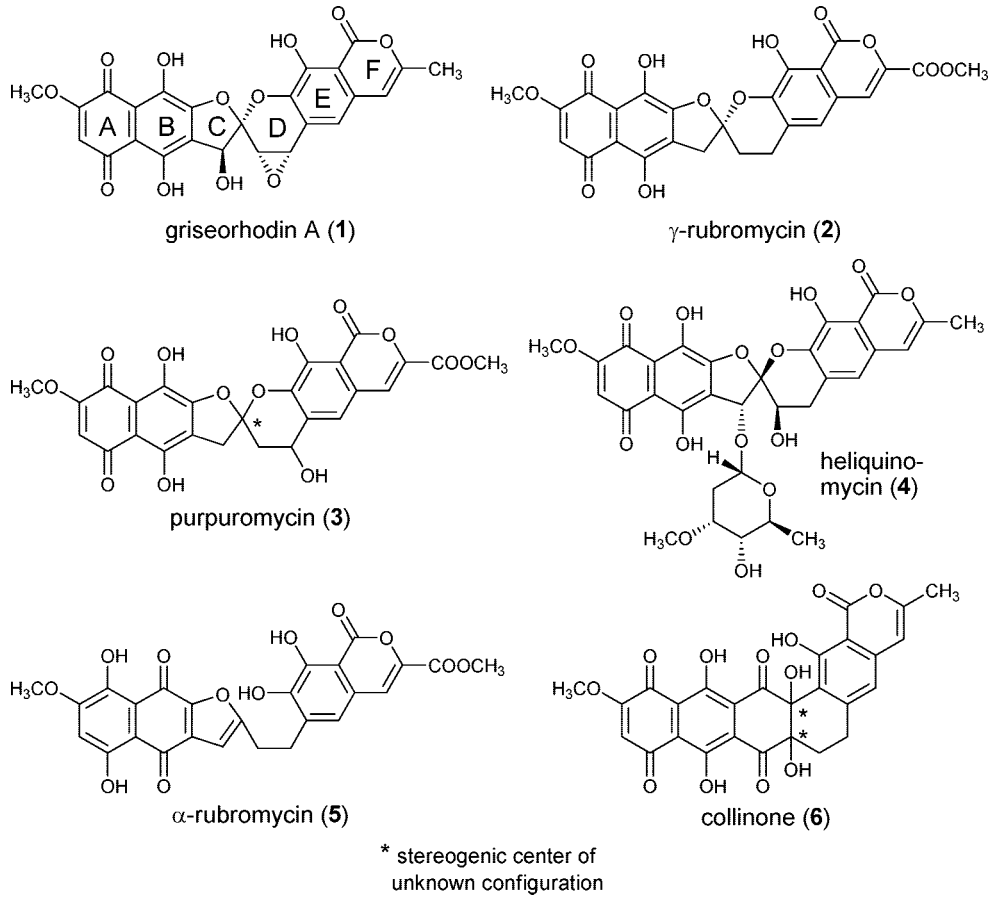

Figure 1. Structures of some members of rubromycin family.

oxyspiroketal unit.[9] The genes were obtained from *Streptomyces* sp. JP95 associated with the marine tunicate *Aplidium lenticulum* and belong to a type-II polyketide synthase (PKS) pathway with an unusually large number of diverse oxidoreductases. One identified key enzyme is the flavin adenine dinucleotide (FAD)-dependent oxidoreductase GrhO5. Removing its gene from the *grh* cluster produced the non-natural pentangular antibiotic collinone (**6**), which carries two more carbon atoms than the biosynthetic end product.[10] Compound **6** was first reported from heterologous expression of an uncharacterized DNA fragment of the rubromycin producer *Streptomyces collinus*, indicating that it is a common intermediate in all rubromycin-type pathways.[11] These data suggested not only that two carbon atoms are excised in a highly unusual fashion to construct the spiroketal pharmacophore but also that rubromycin-type PKSs are rare examples of tridecaketide synthases that generate some of the longest continuous poly-β-keto chains known.[12] To gain deeper insight into this intriguing pathway, in this work we focused on the biosynthetic steps downstream of GrhO5 to investigate how the spiro system is formed. Heterologous expression of 14 modified gene clusters revealed that the pharmacophore is generated in a highly complex oxidative tailoring process involving at least four carbon−carbon bond cleavages.

Results and Discussion

Since all previous attempts to introduce DNA into the griseorhodin producer for genetic modification had failed, we conducted our functional studies in the heterologous expression host *Streptomyces albus* sp. J1074.[13] The cosmid pMP31 carries the entire *grh* cluster in the *Escherichia coli*−*Streptomyces* shuttle vector pAY1.[9] This allowed us to integrate either the whole cluster or engineered variants into the *S. albus* genome. We selected for further studies 14 proteins that either exhibited similarity to oxidoreductases or occurred only in the griseorhodin[9] and rubromycin (GenBank accession no. AF293355) gene clusters (Table 1). Inactivation of the corresponding genes was performed by λ Red-mediated recombination[14,15] on pMP31. Using primers specific for flanking *grh* gene regions and employing as a template plasmid pIJ778, which harbors the spectinomycin resistance gene *aadA*, yielded recombination cassettes that were subsequently electroporated into *E. coli* containing pMP31. Spectinomycin-resistant clones carrying the *aadA* gene instead of the target gene were selected, and the resistance gene was subsequently removed by FLP-mediated excision or *Spe*I restriction and religation. In this way, 14 target variants of the *grh* cluster were obtained, each carrying a deletion of one individual gene. Each gene cluster was

(9) Li, A. Y.; Piel, J. *Chem. Biol.* **2002**, *9*, 1017–1026.
(10) Lackner, G.; Schenk, A.; Xu, Z.; Reinhardt, K.; Yunt, Z. S.; Piel, J.; Hertweck, C. *J. Am. Chem. Soc.* **2007**, *129*, 9306–9312.
(11) Martin, R.; Sterner, O.; Alvarez, M. A.; de Clercq, E.; Bailey, J. E.; Minas, W. *J. Antibiot.* **2001**, *54*, 239–249.
(12) Hertweck, C.; Luzhetskyy, A.; Rebets, Y.; Bechthold, A. *Nat. Prod. Rep.* **2007**, *24*, 162–190.
(13) Chater, K. F.; Wilde, L. C. *J. Gen. Microbiol.* **1980**, *116*, 323–334.
(14) Murphy, K. C.; Campellone, K. G.; Poteete, A. R. *Gene* **2000**, *246*, 321–330.
(15) Datsenko, K. A.; Wanner, B. L. *Proc. Natl. Acad. Sci. U.S.A.* **2000**, *97*, 6640–6645.

Table 1. MS Analysis of Griseorhodin Deletion Mutants (Only Major Compounds Are Shown)

strain	deleted ORF	putative protein function	measured *m/z* $[M + H]^+$	compound	predicted molecular formula
JP95[a]	−	−	509.0720	**1**	$C_{25}H_{16}O_{12}$
MP31[b]	−	−	509.0720	**1**	$C_{25}H_{16}O_{12}$
KR13	*grhD*	thioesterase	509.0717	**1**	$C_{25}H_{16}O_{12}$
KR27	*grhH*	unknown	509.0720	**1**	$C_{25}H_{16}O_{12}$
KR4	*grhI*	unknown	509.0717	**1**	$C_{25}H_{16}O_{12}$
KR39	*grhO2*	ketoreductase	509.0720	**1**	$C_{25}H_{16}O_{12}$
KR23	*grhN*	unknown	509.0711	**1**	$C_{25}H_{16}O_{12}$
KR43	*grhO3*	cytochrome P450	495.0922	**7**	$C_{25}H_{18}O_{11}$
KR7	*grhO7*	NADPH:quinone oxidoreductase	495.0922	**7**	$C_{25}H_{18}O_{11}$
KR42	*grhJ*	GCN5-related *N*-acetyltransferase family	493.0769	**10**	$C_{25}H_{16}O_{11}$
			521.0716	**9**	$C_{26}H_{16}O_{12}$
			457.0921	**11**	$C_{26}H_{16}O_8$
MP66	*grhO6*	FAD-dependent oxygenase	337.0550	**12**	$C_{15}H_{12}O_9$
			521.0720	**9**	$C_{26}H_{16}O_{12}$[c]
KR8	*grhO5*	FAD-dependent oxygenase	535.0877	**6**	$C_{27}H_{18}O_{12}$
KR53	*grhO9*	FAD-dependent oxygenase	505.1120	**13**	$C_{27}H_{21}O_{10}$
KR15	*grhP*	amidotransferase	491.0975	**14**	$C_{26}H_{18}O_{10}$
			507.0922	**15**	$C_{26}H_{18}O_{11}$
KR11	*grhO8*	FAD-dependent oxygenase	477.1150	**16**	$C_{26}H_{20}O_9$
KR41	*grhM*	unknown	461.1240	**17**	$C_{26}H_{20}O_8$
KR5	*grhO1*	oxygenase with covalently bound FAD	n.d.[d]	−	n.d.[d]

[a] Wild-type griseorhodin producer. [b] *S. albus* carrying the entire *grh* cluster. [c] Modified fermentation and extraction protocol. [d] Polyketides were found to bind irreversibly to chromatographic stationary phases.

transferred by conjugation into *S. albus*, and the resulting 14 strains carrying the clusters stably integrated into the genomic *attB* site were grown in liquid LB or TSB medium and on 2CM agar plates[9] for polyketide production.

To obtain evidence indicating which of the deleted genes are involved in the late tailoring steps, we analyzed all of the extracts by liquid chromatography−high-resolution mass spectrometry (LC−HRMS) (Table 1 and Table S1 in the Supporting Information). Table 1 shows the molecular formulas of the main components in each extract, as deduced from the high-resolution masses. The polyketides of the *grhO1* mutant could not be analyzed. Their black color suggested polymerization, and they bound irreversibly to all of the tested chromatographic phases. Variation of cultivation media or extracting plates instead of liquid cultures did not improve this situation.

Surprisingly, five mutants produced a metabolic pattern virtually identical to that of *S. albus* MP31 harboring the entire *grh* cluster, with **1** as the main polyketide. Three of the translated open reading frames (ORFs) that were deleted in these strains did not resemble other proteins, while GrhD and GrhO2 showed similarities to thioesterases and ketoreductases, respectively. The putative proteins might be either without function or redundant, or else the deleted DNA was noncoding. The remaining eight mutants were tentatively placed into two biosynthetic groups according to the number of carbon and oxygen atoms of the polyketides. Our rationale was that the level of oxygenation should increase en route to **1** and that all of the precursors of the advanced uncleaved tridecaketide intermediate **6** should contain 26 or 27 carbons, depending on O-methylation. We identified one series of compounds, generated by the *grhM*, *grhO8*, *grhO9*, and *grhP* mutants, that contained a much smaller number of oxygen atoms (7−10) than **6** (12 oxygens), consistent with an upstream biosynthetic position. Notably, most of these metabolites contained 26 carbons, suggesting that O-methylation of the tridecaketide core system occurs at a late step, shortly before **6** is produced. The second group, which resulted from deletion of *grhO7*, *grhO3*, and *grhJ*, carried a similar number of oxygens as **6** and 25−26 carbon atoms. These highly oxygenated compounds represented convincing candidates for epoxyspiroketal formation and were therefore selected for further studies. An unusual deviation is the *grhO6* mutant, which produced a main compound with a deduced molecular formula of only $C_{15}H_{12}O_9$. For reasons outlined below, this strain was also included into the putative late-tailoring group.

Extracts of mutant KR7 lacking the putative NADPH:quinone oxidoreductase gene *grhO7* contained only a single aromatic polyketide, as judged from HPLC analysis. To characterize the substance, the strain was grown in 6 L of LB medium, and acidified cultures were extracted. Subsequent purification by column chromatography on NaH_2PO_4-impregnated silica yielded 16 mg of a red metabolite. Structure elucidation by one- (1D) and two-dimensional (2D) NMR revealed that the polyketide is dideoxygriseorhodin C (**7**, Figure 2), a known natural product first described from *Streptomyces* sp. No. 76.[16] Compound **7** differs from **1** only by the absence of the epoxide moiety, thus establishing that GrhO7 was involved in the installment of this unit. To our knowledge, epoxidations catalyzed by NADPH: quinone oxidoreductases have not been reported previously. Rather, these proteins and other members of the medium-chain dehydrogenase/reductase superfamily perform nonoxygenative electron-transfer reactions.[17] Examples from aromatic polyketide biosynthesis are the enoylreductases ActVI-ORF2[18] and Med-ORF9[19] from the actinorhodin and medermycin pathways, respectively, which are the closest characterized homologues. We therefore speculated whether the epoxide might be introduced in a two-step process consisting of an initial dehydrogenation of **7** and subsequent double-bond epoxidation by another enzyme. Epoxidations are common reactions of the P450 family,[20,21] and GrhO3 was therefore the most likely candidate for the second step. Surprisingly, analysis of the *grhO3* mutant

(16) Suetsuna, K.; Osajima, Y. *Agric. Biol. Chem.* **1989**, *53*, 241–242.
(17) Riveros-Rosas, H.; Julian-Sanchez, A.; Villalobos-Molina, R.; Pardo, J. P.; Pina, E. *Eur. J. Biochem.* **2003**, *270*, 3309–3334.
(18) Taguchi, T.; Itou, K.; Ebizuka, Y.; Malpartida, F.; Hopwood, D. A.; Surti, C. M.; Booker-Milburn, K. I.; Stephenson, G. R.; Ichinose, K. *J. Antibiot.* **2000**, *53*, 144–152.
(19) Ichinose, K.; Ozawa, M.; Itou, K.; Kunieda, K.; Ebizuka, Y. *Microbiology* **2003**, *149*, 1633–1645.
(20) Guengerich, F. P. *Arch. Biochem. Biophys.* **2003**, *409*, 59–71.
(21) Grüschow, S.; Sherman, D. H. In *Aziridines and Epoxides in Organic Synthesis*; Yudin, A. K., Ed.; Wiley-VCH: Weinheim, Germany, 2006.

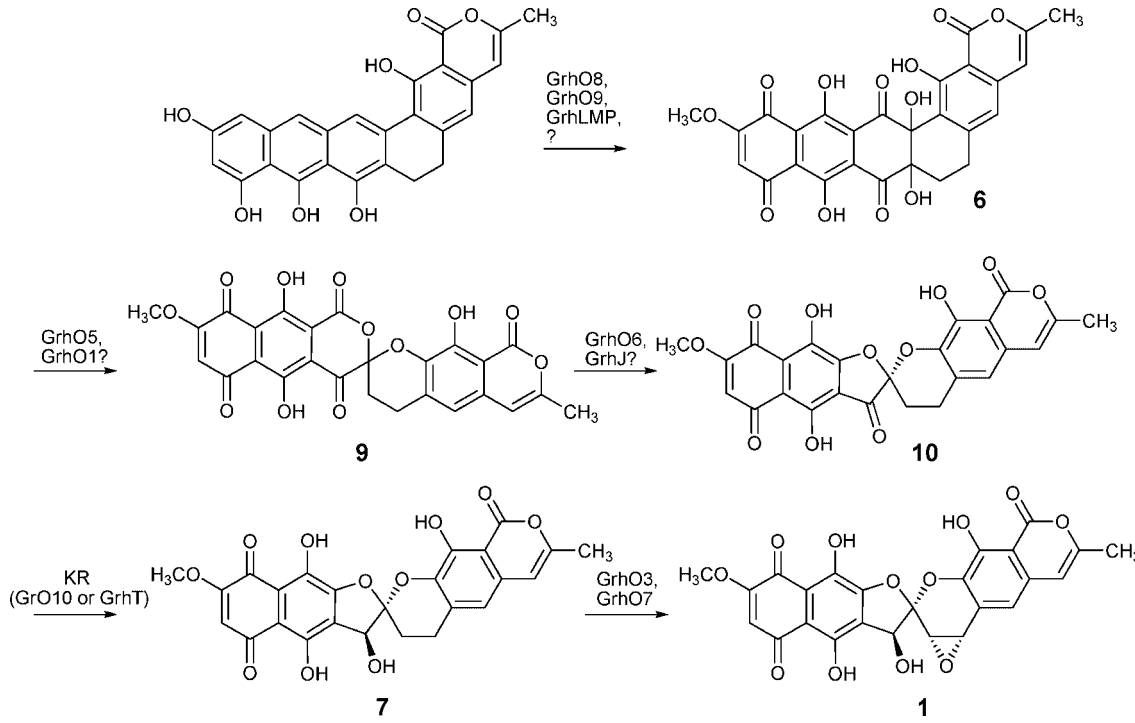

Figure 2. Current model of the griseorhodin A (**1**) biosynthetic pathway.

KR43 again revealed a single metabolite that was identical with **7**. From these data, one can conclude that GrhO7 and GrhO3 jointly participate in epoxide formation, but the production of an identical substance by the two mutants was unexpected. A possible explanation is that the two enzymes form a complex that is inactive if one component is removed. Either the components could epoxidize **7** via a tightly bound olefinic intermediate, or GrhO3 could directly generate the epoxide from the single bond, in which case GrhO7 might then be responsible for the reductive recycling of olefinic shunt products that arise from an eliminative side reaction. Although cytochromes P450 usually generate epoxides from alkenes,[21] examples of the formation of cyclic ethers from saturated precursors have been reported, such as the epoxidase OleP from oleandomycin biosynthesis[22] and the aureothin P450 AurH, which closes a tetrahydrofuran ring by 1,5-dehydrogenation of an alcohol precursor.[23] Another possibility is that the true substrate of GrhO7 is not **7** but that it spontaneously reacts with this compound in the absence of the enzyme. In order to search for such a genuine precursor, we tested several alternative cultivation and isolation conditions but could not detect compounds other than **7**.

Among the closest homologues of GrhO6 are MtmOIV[24] and CmmOIV,[25] which perform Baeyer−Villiger-type reactions in the mithramycin and chromomycin pathways, respectively. GrhO6 therefore represented a prime candidate to be an enzyme directly involved in spiroketal formation by carbon−carbon bond cleavage. When extracts of the *grhO6* mutant *S. albus* MP66 were initially analyzed by LC−MS, numerous pigmented compounds were detected in small quantities, suggesting that the substrate of GrhO6 is unstable. The main component of this mixture was isolated, and HRMS measurements confirmed the unusually small molecular ion previously also observed by HPLC−electrospray ionization (ESI)-MS analysis, matching the molecular formula $C_{15}H_{12}O_9$. According to carbon and proton chemical shifts (Table 2) and heteronuclear multiple bond correlation (HMBC) correlations (Figure 3), 11 of the 15 carbons and 6 of the 12 protons could be assigned to a spin system that is identical to the methoxylated quinoid AB ring in **1**. All six remaining protons resonated at 3.87 ppm, indicating that they belonged to two methoxy groups; this result, together with two pairs of almost overlapping carbon signals at ~164.8 and 53.8 ppm, established the presence of two methyl ester functions. These were connected to C2 and C11 via HMBC couplings, identifying the substance as a novel naphthoquinone, ZY1 (**8**), that lacks the entire eastern half of the griseorhodin-type compounds. In accordance with this structure, no NMR signals for the EF ring system present in those polyketides and in **6** were observed. It was initially surprising that inactivation of a putative cleaving enzyme would lead to a more heavily fragmented product. We suspected that the two methyl ester groups present in **8** might be an artifact generated from methanol used during workup. Omission of methanol from this procedure indeed resulted in the disappearance of **8** but did not reduce the complexity of the metabolic mixture. However, by carefully adjusting fermentation and isolation, we were able to substantially reduce unwanted decomposition reactions. This allowed us to isolate 20 mg of a new main compound, lenticulone (**9**), from a scaled-up 12 L culture of this strain. HR-ESI-MS measurements were consistent with the molecular formula $C_{26}H_{16}O_{12}$ (*m/z* 521.0714 measured, 521.0715 calcd for $[M + H]^+$). ^{13}C NMR analysis (Table 2) confirmed the presence of 26 carbon atoms, which is one carbon more than in **1**. Evaluation of the 1D and 2D NMR data allowed for an assignment of all of the C and H signals. The spectra closely resembled those of

(22) Shah, S.; Xue, Q.; Tang, L.; Carney, J. R.; Betlach, M.; McDaniel, R. *J. Antibiot.* **2000**, *53*, 502–508.
(23) He, J.; Müller, M.; Hertweck, C. *J. Am. Chem. Soc.* **2004**, *126*, 16742–16743.
(24) Gibson, M.; Nur-e-alam, M.; Lipata, F.; Oliveira, M. A.; Rohr, J. *J. Am. Chem. Soc.* **2005**, *127*, 17594–17595.
(25) Menendez, N.; Nur-e-Alam, M.; Brana, A. F.; Rohr, J.; Salas, A. F.; Mendez, C. *Chem. Biol.* **2004**, *11*, 21–32.

Table 2. NMR Data for ZY1 (**8**) and Lenticulone (**9**)

	ZY1 (**8**)		lenticulone (**9**)	
position	^{13}C	^{1}H	^{13}C	^{1}H
1	164.76		158.28	
2	132.58		121.74	
3	154.06		155.88	
4	115.1		118.26	
5	184.35		181.67	
6	162.44		161.15	
7	111.53	6.34 (s, 1H)	110.20	6.29 (s, 1H)
8	190.13		188.78	
9	114.52		117.93	
10	153.12		153.61	
11	130.77		127.7	
12	164.82		182.81	
13			99.08	
14			23.96	2.4−2.5 (m, 2H)
15a			20.59	3.25 (m, 1H)
15b			20.59	2.85 (ddd, *J*= 2.7, 5.52, 17.2 Hz, 1H)
16			132.09	
17			114.21	6.61 (s, 1H)
18			131.39	
19			104.01	6.17 (s, 1H)
20			152.85	
21			166.66	
22			105.08	
23			150.15	
24			137.14	
25			19.30	2.24 (s, 3H)
1−OMe	53.82	3.87 (s, 1H)		
6−OMe	58.18	3.93 (s, 1H)	57.33	4.01 (s, 3H)
12−OMe	53.82	3.87 (s, 1H)		
3−OH		12.16 (s, 1H)		12.74 (s, 1H)
10−OH		12.87 (s, 1H)		13.37 (s, 1H)
23−OH				10.98 (s, 1H)

7, and in particular, both the methoxylated naphthoquinone and the methylated benzopyrone spin system connected with an ethylene group could be identified. One carbon signal at 99.08 ppm, which is characteristic for a (hemi)acetal function, showed an HMBC coupling to protons from the two ethylene carbons (Figure 3), suggesting that the compound contains a spiro system at a position analogous to that of the spiro center in **1**. In comparison with **7**, two new signals in the carbonyl region were identified at 158.28 (C1) and 182.81 ppm (C12), while a signal corresponding to the secondary alcohol function of **7** was absent. HMBC couplings of the C3−OH proton with C1 connected this carbonyl group to C2 of the B ring. Couplings of the C14−CH_2 protons (2.4−2.5 ppm) with C12 and the downfield shift of the C12 signal indicated that an additional keto function was positioned adjacent to the acetal carbon. This suggested the structure for **9** shown in Figure 3. For additional support for the constitution, the compound was fragmented by HR-ESI-MS/MS (Figure 4 and Table S1 in the Supporting Information). Besides losses of small neutral molecules, which were not structurally indicative, collision-induced dissociation (CID) of the sodium adduct ion $[M + Na]^+$ yielded one major fragment with an exact mass difference Δm of 204.0372, indicating a loss of $C_{11}H_8O_4$. This was assigned to a cleavage of ring D (Figure 4, fragmentation path A**),** resulting in the formation of the ion $[I + Na]^+$. In addition, $[II + Na]^+$ ($\Delta m = 316.0155$; loss of $C_{15}H_8O_8$) was observed, although at smaller abundance. Two other fragmentation products were of diagnostic value because they could be assigned to a cleavage of ring C of **9** (Figure 4, path B): loss of $C_{13}H_6O_7$ (III, $\Delta m = 246.0362$) and $C_{13}H_{10}O_5$ (IV, $\Delta m = 274.0054$). An MS^3 experiment with the main product ion $[I + Na]^+$ showed only water expulsion. Therefore, a hypothetical alternative formation of $[III + Na]^+$ by subsequent fragmentation of $[I + Na]^+$ could be ruled out. Direct fragmentation of **9** can lead to $[III + Na]^+$ only if the constitution of ring C is the one shown in Figure 3, i.e., the carbonyl function at C12 must be connected to ring B. Thus, the MS^n data confirmed that **9** is a novel spiroketal containing a ring C that is expanded in comparison with those in the griseorhodins and rubromycins.

The presence of an additional carbon−carbon bond in **9** compared with **1** suggests that GrhO6 has the critical function in the installation of the spiroketal system of cleaving the C1−C2 bond in **9**. While a number of Bayer−Villigerases have been reported,[26] GrhO6 would be an unusual example of a monooxygenase acting on an ester instead of a ketone (Figure 5, route A). However, although the high protein similarity to Baeyer−Villigerases suggests a related chemistry, carbon-bond cleavage could also be rationalized by an alternative route involving ring hydroxylation (Figure 5, route B) and subsequent fragmentation aided by rearomatization. A related mechanism has been proposed for 4-hydroxybenzoate hydroxylase on the basis of inhibitor studies and molecular orbital considerations.[27] Fraaije et al.[28] have previously reported a Trp residue in a conserved FxGxxxHxxxW motif that would distinguish Bayer−Villigerases from the other flavin-containing monooxygenases, but neither the motif of GrhO6 nor of the closely related mithramycin and chromomycin Bayer−Villigerases contain this amino acid. Functional studies are therefore needed to establish the exact mechanism of GrhO6. So far, biochemical experiments with the overexpressed and purified enzyme were not met with success because of the extremely low solubility and short half-life of **9** under all tested assay conditions. However, it should be intriguing to study GrhO6 with model compounds in order to assess its potential for the development of novel chemoenzymatic transformations.

GrhJ shows homology to GCN5-related *N*-acetyltransferases (GNATs). The occurrence of such enzymes in aromatic polyketide pathways has to our knowledge not been reported to date, but type-I PKSs sometimes use GNATs to incorporate acetyl starter units into complex polyketides.[29,30] We therefore initially suspected that GrhJ plays a similar role in starter-unit incorporation and might be needed for the formation of the unusually long tridecaketide chain. However, examination of the knockout mutant KR42 revealed a series of highly oxygenated compounds, the most prominent of which was isolated and identified as **9**. This suggested that GrhJ together with GrhO6 catalyzes the final steps of spiroketal formation. In addition to **9**, a polyketide with the molecular formula $C_{25}H_{16}O_{11}$ was observed by LC−HRMS analysis of a plate culture. This compound, which was not detectable in the GrhO6 mutant, contains one less carbon atom and one less oxygen atom than **9** and could be identical to the postulated cleavage product 7,8-dideoxy-6-oxygriseorhodin C (**10**) (Figure 5). Unfortunately, the amounts produced were too small for a full characterization by NMR. Further examination of GrhJ will be highly interesting,

(26) Mihovilovic, M. D. *Curr. Org. Chem.* **2006**, *10*, 1265–1287.
(27) Eppink, M. H. M.; Boeren, S. A.; Vervoort, J.; VanBerkel, W. J. H. *J. Bacteriol.* **1997**, *179*, 6680–6687.
(28) Fraaije, M. W.; Kamerbeek, N. M.; van Berkel, W. J. H.; Janssen, D. B. *FEBS Lett.* **2002**, *518*, 43–47.
(29) Piel, J.; Wen, G.; Platzer, M.; Hui, D. *ChemBioChem* **2004**, *5*, 93–98.
(30) Gu, L. C.; Geders, T. W.; Wang, B.; Gerwick, W. H.; Hakansson, K.; Smith, J. L.; Sherman, D. H. *Science* **2007**, *318*, 970–974.

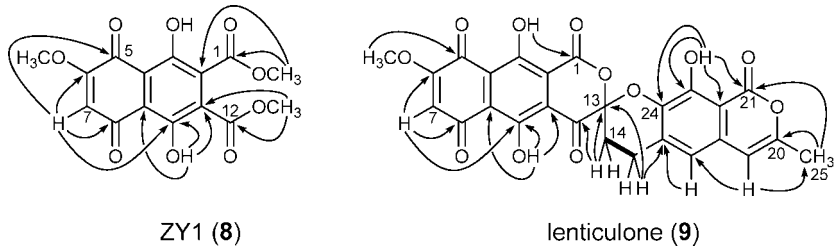

Figure 3. Structures and key HMBC (arrows) and $^{1}H-^{1}H$ COSY (bold line) correlations of ZY1 (**8**) and lenticulone (**9**).

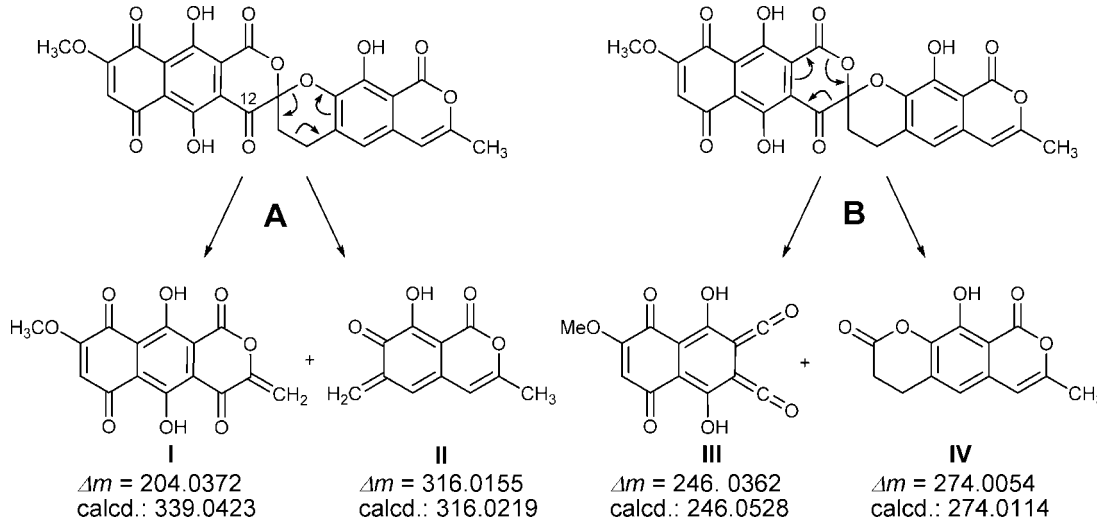

Figure 4. MS/MS fragmentation pathways for lenticulone (**9**). The measured and calculated mass differences of the $[M + Na]^{+}$ ions are shown below the respective fragmentation products.

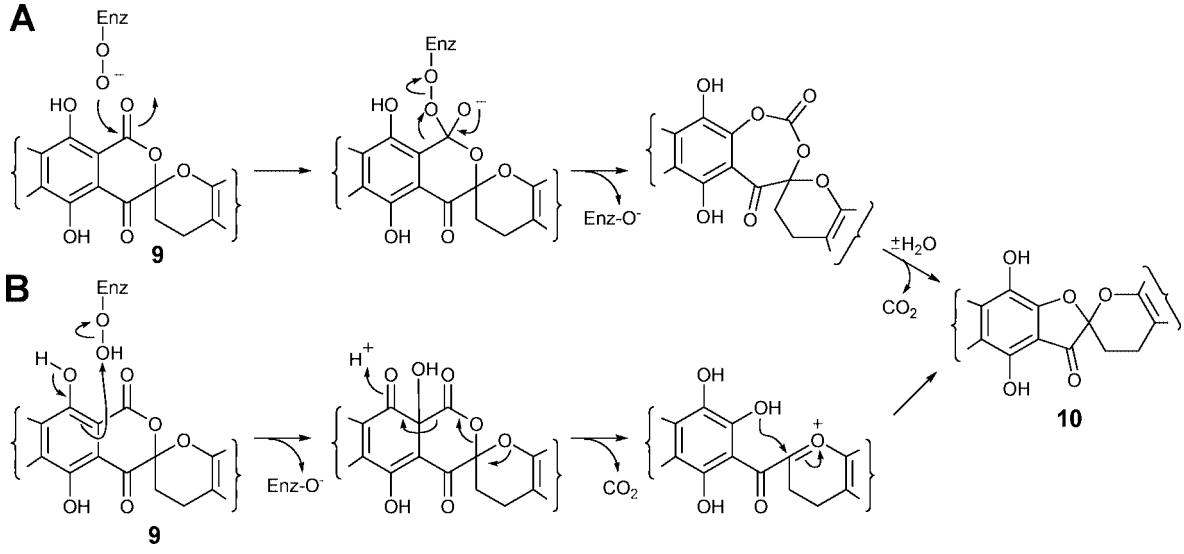

Figure 5. Two possible pathways for the final carbon−carbon bond cleavage in griseorhodin A biosynthesis (only the B, C, and D rings are shown): (A) GrhO6 acts as a Baeyer−Villigerase on the ester moiety of **9**, resulting in decarboxylation; (B) GrhO6 hydroxylates the ester α-position, and decarboxylation results from rearomatization.

since the catalysis of a polyketide tailoring reaction is unprecedented GNAT chemistry.[31]

Taken together, the gene deletion experiments suggest an updated biosynthetic pathway for griseorhodin A biosynthesis, as shown in Figure 2. By a set of early tailoring enzymes, an initial cyclized tridecaketide intermediate assembled from one acetyl-CoA and twelve malonyl-CoA units is converted into the advanced uncleaved precursor **6**. Subsequently, three carbon−carbon bonds are cleaved to yield **9**. According to previous knockout experiments,[10] the FAD-dependent oxidoreductase GrhO5 should immediately act on **6** to generate an as yet unidentified product. It is unlikely that all three cleavages are performed by a single enzyme. The oxygenase GrhO1 with covalently bound FAD,

(31) Vetting, M. W.; de Carvalho, L.; Yu, M.; Hedge, S. S.; Magnet, S.; Roderick, S. L.; Blanchard, J. S. *Arch. Biochem. Biophys.* **2005**, *433*, 212–226.

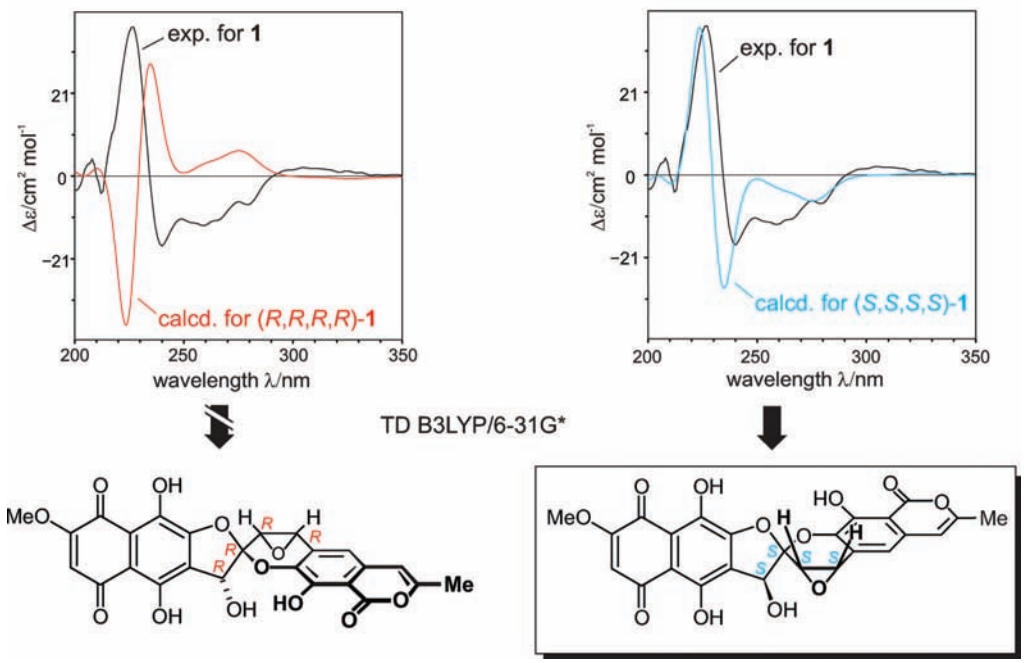

Figure 6. Attribution of the absolute configuration of griseorhodin (**1**) by comparison of the CD spectra calculated for its two enantiomers with the experimental spectrum.

Table 3. Pharmacological Data for Collinone (**6**), Lenticulone (**9**), Dideoxygriseorhodin C (**7**), and Griseorhodin A (**1**)

	antiproliferative activity		cytotoxicity	antibacterial activity		HLE inhibition
compound	Huvec GI_{50} (μmol mL^{-1})	K-562 GI_{50} (μmol mL^{-1})	HeLa CC_{50} [CC_{10}] (μmol mL^{-1})	*S. carnosus* MIC (μmol mL^{-1})	*B. subtilis* MIC (μmol mL^{-1})	IC_{50} (μM)[a]
6	64×10^{-3}	37×10^{-3}	63×10^{-3} [23×10^{-3}]	10×10^{-3}	5×10^{-3}	8.91 ± 1.87
9	96×10^{-3}	35×10^{-3}	90×10^{-3} [42×10^{-3}]	43×10^{-3}	10×10^{-3}	2.68 ± 0.59
7	87×10^{-3}	73×10^{-3}	78×10^{-3} [29×10^{-3}]	0.5×10^{-3}	8×10^{-6}	1.40 ± 0.32
1	44×10^{-3}	38×10^{-3}	60×10^{-3} [17×10^{-3}]	2.8×10^{-3}	25×10^{-6}	1.88 ± 0.17

[a] IC_{50} values were obtained from duplicate (**6**, **1**) or triplicate (**9, 7**) measurements with five different inhibitor concentrations and linear-regression analysis using the equation $v = v_0(1 + [I]/IC_{50})$, where v_0 is the rate in the absence of the inhibitor and [I] is the inhibitor concentration.

homologues of which can catalyze unusual chemistry in polyketide biosynthesis,[32] is a candidate for further conversion to **9**. However, this remains to be validated, since the intermediates accumulated by *grhO1* deletion mutants are highly labile and difficult to analyze. In **9**, one further carbon−carbon bond is cleaved by the Baeyer−Villigerase-like GrhO6, very likely in cooperation with the GNAT GrhJ, to establish the spiroketal moiety. After keto reduction, the biosynthesis is completed by joint action of P450 GrhO3 and NADPH:ubiquinone oxidoreductase GrhO7, which epoxidize the saturated bond at C14−C15.

Since our data suggested that GrhO6 and GrhJ introduce a chiral dioxaspirodecane moiety, we set out to determine the hitherto unknown absolute configuration of **1**. In previous derivatization experiments, Eckardt et al.[33] had established the relative configuration of **1** as shown in Figure 1. Interestingly, work on the stereochemistry of heliquinomycin (**4**) and the rubromycins using quantum-chemical circular dichroism (CD) calculations had demonstrated that the spiro center is configured differently in these closely related compounds.[34] To establish the absolute configuration of **1**, a conformational analysis based on the above-mentioned relative configuration was performed using density functional theory (DFT) at the B3LYP/6-31G* level[35−38] These calculations yielded three conformers within an energetic range of 3 kcal mol^{-1} and thus in a relevant percentage of the population for subsequent CD investigations. For each conformer, single CD spectra were generated by excited-state time-dependent DFT calculations at the B3LYP/6-31G* level. These were Boltzmann-weighted,[39] giving an overall CD spectrum. After a UV correction[39,40] by 5 nm, comparison of the theoretical spectra with the experimental one revealed an excellent agreement between the theoretical CD curve for (*S*,*S*,*S*,*S*)-**1** and the CD measurements, while the spectrum calculated for the (*R*,*R*,*R*,*R*)-**1** enantiomer was inverted with respect to the experimental curve (Figure 6). The (*S*) configuration of the spiro center in **1** is therefore identical with that in γ-rubromycin (**2**) and opposite to that in **4**.[41]

(32) Xiang, L.; Kalaitzis, J. A.; Moore, B. S. *Proc. Natl. Acad. Sci. U.S.A.* **2004**, *101*, 15609–15614.
(33) Eckardt, K.; Tresselt, D.; Schönecker, B. *Tetrahedron* **1979**, *35*, 1621–1624.
(34) Bringmann, G.; Kraus, J.; Schmitt, U.; Puder, C.; Zeeck, A. *Eur. J. Org. Chem.* **2000**, 2729–2734.
(35) Becke, A. D. *J. Chem. Phys.* **1993**, *98*, 5648–5652.
(36) Lee, C. T.; Yang, W. T.; Parr, R. G. *Phys. Rev. B* **1988**, *37*, 785–789.
(37) Hariharan, P. C.; Pople, J. A. *Theor. Chim. Acta* **1973**, *28*, 213–222.
(38) Francl, M. M.; Pietro, W. J.; Hehre, W. J.; Binkley, J. S.; Gordon, M. S.; Defrees, D. J.; Pople, J. A. *J. Chem. Phys.* **1982**, *77*, 3654–3665.
(39) Bringmann, G.; Busemann, S. In *Natural Product Analysis: Chromatography, Spectroscopy, Biological Testing*; Schreier, P., Herderich, M., Humpf, H.-U., Schwab, W., Eds.; Vieweg: Wiesbaden, Germany, 1998; pp 195−211.
(40) For a first review of the determination of absolute configuration by LC−CD in combination with quantum-chemical calculations, see: Bringmann, G.; Gulder, T. A. M.; Reichert, M.; Gulder, T. *Chirality* **2008**, *20*, 628–642.

To determine how the degree of oxidative modification during griseorhodin biosynthesis affects bioactivity, we tested **6**, **9**, **7**, and **1** in antiproliferative and cytotoxicity assays (Table 3). In general, the activities of all of these compounds were in the same range, with **7** generally being slightly less active in all assays and **9** showing decreased activity only in the Huvec assay. We also tested the compounds for antibiotic properties against *Staphylococcus carnosus* and *Bacillus subtilis* (Table 3). Substance **7** was the most potent polyketide, while the non-natural compound **9** still exhibited good activity. Some oxa-heterocyclic natural products are known to inhibit serine proteases. Examples include the inhibition of trypsin by flavonoids[42,43] and thrombin by triterpene lactones from *Lantana camara*.[44] We evaluated crude extracts of polyketide-producing strains toward the model serine proteases chymotrypsin, trypsin, and human leukocyte elastase (HLE). None of the strains KR4, KR5, KR7, KR8, KR13, KR66, MP31, or MP63 (Table 1) had inhibitory activity against chymotrypsin or trypsin at a concentration of 50 μg mL^{-1}. However, HLE-inhibitory activity was determined for the crude extracts of all strains, with KR7 showing the best activity ($IC_{50} = 3.10 \pm 0.83$ μg mL^{-1}). The activities were confirmed with purified compounds, and the IC_{50} values are given in Table 3. Compound **7**, the polyketide produced by KR7, exhibited the strongest inhibition of HLE. This is, to the best of our knowledge, the first report of HLE-inhibitory activity of aromatic polyketides.

Conclusion

We have been able to identify most, if not all, of the enzymes responsible for spiroketal formation and epoxidation in griseorhodin biosynthesis, revealing a remarkably complex oxidative tailoring process. Various biosynthetic pathways that produce pentangular intermediates structurally related to uncleaved griseorhodin precursors are known.[10,45,46] With the gene information in hand, it will be worthwhile to test whether *grh* tailoring genes can be used to convert these compounds into biologically active new hybrid polyketides carrying the spiroketal pharmacophore.

Experimental Section

General. One- and two-dimensional ^{1}H- and ^{13}C NMR spectra were recorded on Bruker Avance dpx 300 and drx 500 spectrometers, respectively, in DMSO-d_6 or $CDCl_3$ (unless indicated otherwise) using the solvent signals as the references. HR-ESI-MS and CID MS^n spectra were recorded on a Bruker micrOTOF-Q time-of-flight mass spectrometer and a Bruker APEX IV Fourier transform ion cyclotron resonance (FT-ICR) mass spectrometer with a 7.05 T magnet. Both instruments were equipped with an Apollo electrospray ion source. Analyte solutions in acetonitrile were introduced into the ion source with a syringe pump (Cole-Parmer Instruments, Series 74900) at flow rates of 3−4 μL min^{-1} or with an Agilent 1200 series HPLC pump at a flow rate of 50 μL/min. For CID, argon was used as the collision gas. Ion transfer into the first of three differential pumping stages in the ion source occurred through a 0.5 mm i.d. glass capillary with nickel coatings at both ends. Thin layer chromatography was performed on silica gel 60 F_{254} plates (layer thickness 0.2 mm, Merck). Plates were impregnated with aqueous 2 M NaH_2PO_4 solution and subsequently dried. For column chromatography, NaH_2PO_4-impregnated silica gel 60, 40−63 μm (Roth) (for impregnation, the silica gel was stirred for 1 h in aqueous 2 M NaH_2PO_4, after which the aqueous phase was removed by filtration and the silica gel dried at 120 °C for 3 h), or Sephadex LH-20 (bead size 25−100 μm, Sigma) was used. Preparative HPLC separation was performed on a PerfectChrom 100 C18 reversed-phase semipreparative column (250 mm × 8 mm, 5 μm) with a flow rate of 6 mL min^{-1} and analytic HPLC on a PerfectChrom 100 C18 reversed-phase analytic column (250 mm × 4 mm, 5 μm) with a flow rate of 1 mL min^{-1}. The compounds were detected with a Jasco MD-2015 PDA detector at wavelengths of 254 and 488 nm.

Trypsin and chymotrypsin, both from bovine pancreas, were purchased from Sigma-Aldrich (Steinheim, Germany) and Fluka (Deisenhofen, Germany). HLE was obtained from Calbiochem (Darmstadt, Germany). Suc-Ala-Ala-Pro-Arg-pNA, Suc-Ala-Ala-Pro-Phe-pNA, and MeOSuc-Ala-Ala-Pro-Val-pNA were purchased from Bachem (Bubendorf, Switzerland). Enzymatic assays were performed on a Varian Cary 50 Bio spectrophotometer.

Bacterial Strains and Culture Conditions. *S. albus* J1074 (kindly provided by Prof. J. Salas) served as the host strain for heterologous expression experiments. For polyketide production, wild-type and mutant strains were cultivated in LB medium, MS (mannitol soya flour)[47] and TSB (tryptic soy broth) for 4−6 days at 30 °C with shaking. *S. albus* exconjugants were selected with apramycin at 50 μg mL^{-1} or kanamycin at 50 μg mL^{-1} in a solid or liquid medium, depending on the specific requirements. *E. coli* strain XL1 blue served as the host for routine subcloning. For intergeneric conjugation, *E. coli* ET12567 containing the RP4 derivative pUZ8002 was used.[47] *E. coli* strains were grown in LB medium supplemented with ampicillin (100 μg mL^{-1}), apramycin (50 μg mL^{-1}), or streptomycin (50 μg mL^{-1}) for selection.

Plasmids and General DNA Procedures. DNA isolation, plasmid preparation, restriction digests, gel electrophoresis, and ligation reactions were conducted according to standard methods.[47,48] pBluescript II SK(−) and pDH5[49] and SuperCos1 (Stratagene) were the routine vectors for subcloning and preparation of DNA templates for sequencing.

Gene Inactivation. With the exception of the *grhO6* mutant, the in-frame gene-deletion strains were constructed by polymerase chain reaction (PCR)-mediated gene replacement based on the λ Red technology.[14,15] The spectinomycin resistance cassette (*aadA*) flanked by FRT sites was amplified from pIJ778 with two long primers, each comprising 39 nucleotide homology from sense/antisense strands ending in start/stop codons (for the primers used, see Table S2 in the Supporting Information). The extended resistance cassette was electroporated into *E. coli* BW 25113/pIJ790 containing the cosmid pMP31, which carries the entire *grh* biosynthesis gene cluster,[9] with concurrent substitution of the respective gene. Streptomycin-resistant clones were selected and verified by PCR. Subsequently, the antibiotic resistance cassettes were eliminated by FLP-mediated excision in *E. coli* DH5α/BT340,

(41) It should be kept in mind that the absolute configurations determined in refs 3 and 34 are both correct but that the wrong descriptors were used. Thus, the correct configurations at the spiro center are (*S*) for heliquinomycin and (*R*) for γ-rubromycin. In a similar way, the two possible enantiomers of griseorhodin A were given the wrong descriptors at the spiro center in ref 33.

(42) Checa, A.; Ortiz, A. R.; de Pascual-Teresa, B.; Gago, F. *J. Med. Chem.* **1997**, *40*, 4136–4145.
(43) Maliar, T.; Jedinák, A.; Kadrabová, J.; Sturdik, E. *Eur. J. Med. Chem.* **2004**, *39*, 241–248.
(44) Weir, M. P.; Bethell, S. S.; Cleasby, A.; Campbell, C. J.; Dennis, D. J.; Finch, H.; Jhoti, H.; Mooney, C. J.; Patel, S.; Tang, C. M.; Wonacott, M. A.; Wharton, C. W. *Biochemistry* **1998**, *37*, 6645–6657.
(45) Chen, Y. H.; Luo, Y. G.; Ju, J. H.; Wendt-Pienkowski, E.; Rajski, S. R.; Shen, B. *J. Nat. Prod.* **2008**, *71*, 431–437.
(46) Kim, B. C.; Lee, J. M.; Ahn, J. S.; Kim, B. S. *J. Microbiol. Biotechnol.* **2007**, *17*, 830–839.
(47) Kieser, T.; Bibb, M. J.; Buttner, M. J.; Chater, K. F.; Hopwood, D. A. *Practical Steptomyces Genetics*; The John Innes Foundation: Norwich, U.K., 2000.
(48) Sambrook, J.; Russel, D. W. *Molecular Cloning: A Laboratory Manual*, 3rd ed.; Cold Spring Harbor Laboratory Press: Cold Spring Harbor, NY, 2001.
(49) Hillemann, D.; Pühler, A.; Wohlleben, W. *Nucleic Acids Res.* **1991**, *19*, 727–731.

leaving an 81 base pair (bp) "scar" sequence, or by *Spe*I restriction and religation, leaving only one *Spe*I site. The resulting cosmids (pKR5 for the *grhO1*, pKR39 for the *grhO2*, pKR43 for the *grhO3*, pKR8 for the *grhO5*, pKR7 for the *grhO7*, pKR11 for the *grhO8*, pKR53 for the *grhO9*, pKR13 for the *grhD*, pKR27 for the *grhH*, pKR4 for the *grhI*, pKR42 for the *grhJ*, pKR41 for the *grhM*, pKR23 for the *grhN*, and pKR15 for the *grhP* deletion) were individually introduced into *S. albus* J1074 by conjugation using *E. coli* ET12567/pUZ8002. Apramycin-resistant exconjugants were selected, and the correct integration event was checked by PCR on genomic DNA isolated from the strains.

To remove *grhO6*, a different strategy was used. From the plasmids no. 52 and no. 122, obtained by shotgun subcloning of pMP31 in pBluescript SKII(−), a 800 bp *Sma*I-*Bam*HI fragment and a 1300 bp *Bam*HI-*Hin*dIII fragment, respectively, covering the regions upstream and downstream of *grhO6* were excised. These were ligated into pDH5 digested with *Sma*I and *Hin*dIII to give pMP53. To obtain the *neo* kanamycin resistance cassette, SuperCos1 was restricted with *Sma*I/*Hin*dIII. The *Hin*dIII end was filled with Klenow enzyme and the fragment ligated into the *Sma*I-restricted pIJ4642 to give pMP64. Next, the *neo BamHI* fragment was inserted into the *Bam*HI site of pMP53, resulting in pMP65. The fragment was excised with *Sma*I/*Hin*dIII and electroporated into *E. coli* BW 25113/pIJ790 containing pMP31 to substitute *grh*O6. After selection with kanamycin, the cosmid derivative pMP66 was reisolated from positive clones and introduced into *S. albus* J1074 by conjugation from *E. coli* ET12567/pUZ8002, yielding mutant strain *S. albus* MP66.

Production, Isolation, and Analysis of Didesoxygriseorhodin C (7). *S. albus* KR7 spores were inoculated into 100 mL of LB medium and grown overnight. The resultant seed culture was used to inoculate 6 L of LB medium distributed to 15 baffled 1 L flasks. The flasks were incubated at 220 rpm for 6 days at 30 °C. For compound isolation, the mycelia were harvested by centrifugation and suspended in 300 mL of dH_2O, and the pH of the mixture was adjusted to 3−4 with trifluoroacetic acid (TFA). After extraction with 3 × 200 mL of EtOAc, the combined extracts were fractionated by flash column chromatography on impregnated silica (9:1 $CHCl_3$/MeOH). Fractions containing **7** were combined, dried, and further chromatographed by semipreparative HPLC (gradient: 25 to 90% CH_3CN in H_2O with 0.1% TFA over 25 min), yielding 16 mg of pure compound. The molecular formula was deduced by HR-ESI-MS analysis as $C_{25}H_{18}O_{11}$ (*m*/*z* 494.089 measured, 494.085 calcd for $[M + H]^+$). The identity of the compound was confirmed by 1D and 2D NMR analysis (DMSO-d_6). All of the spectral data were identical with the data in the literature.[16]

Production, Isolation, and Analysis of ZY1 (8). *S. albus* MP66 was grown in 12 L of LB medium distributed to 500 mL Erlenmeyer flasks with stainless-steel springs; each flask contained 200 mL of culture. The flasks were incubated at 200 rpm for 4 days at 30 °C. Mycelia were harvested by centrifugation and suspended in 400 mL of dH_2O. After adjustment to pH 2 with 2 N HCl, the mixture was extracted with 3 × 300 mL of 95:5:1 EtOAc/MeOH/AcOH. The combined extracts were fractionated by flash column chromatography on impregnated silica (9:1 $CHCl_3$/MeOH). Fractions containing the compound were combined and dried, and further purification was carried out by gel filtration using Sephadex LH-20 gel filtration (MeOH). After evaporation of the solvent, 12 mg of **8** was obtained. NMR data for **8** are given in Table 2. HRMS for $[M + H]^+$ of $C_{15}H_{12}O_9$: *m*/*z* 337.055 found, 337.056 calcd. UV (acetonitrile) ν: 490, 362, 310, 260 nm.

Production, Isolation, and Analysis of Lenticulone (9). *S. albus* MP66 was grown in 12 L of LB medium distributed to 1 L baffled flasks; each flask contained 400 mL of culture for production. After incubation at 220 rpm for 4 days at 30 °C, the cells were harvested by centrifugation and suspended in 400 mL of dH_2O. The solution was acidified to pH 3−4 with TFA and extracted with 3 × 300 mL of EtOAc. To prevent decomposition of **9** during solvent removal, TFA was back-extracted with dH_2O. The crude extract was fractionated by flash column chromatography on impregnated silica (5:1 $CHCl_3$/EtOAc). Fractions containing the compound were combined and dried, and further purification was carried out by semipreparative HPLC (gradient: 25 to 100% CH_3CN in H_2O with 0.1% TFA over 25 min). The isolated yield of **9** was 20 mg. NMR data for **9** are given in Table 2. IR ν: 2923, 2853, 1686, 1650,1606, 1438, 1403, 1336, 1289, 1234, 1197, 1145, 1069, 1053, 1006, 989, 932, 893, 857, 819, 799, 747, 697, 668, 585, 568, 546, 519, 445, 421, 412 cm^{-1}. UV (acetonitrile) ν: 494, 355, 230 nm. HRMS for $[M + H]^+$ of $C_{26}H_{16}O_{12}$: *m*/*z* 521.0714 found, 521.0720 calcd. MS−MS fragmentation data: see Table S1 in the Supporting Information.

HLE Inhibition Assay. HLE was assayed spectrophotometrically at 405 nm at 25 °C. The assay buffer was 50 mM sodium phosphate buffer containing 500 mM NaCl (pH 7.8). A 50 μg mL^{-1} enzyme stock solution was prepared in 100 mM sodium acetate buffer (pH 5.5) and diluted with assay buffer. Stock solutions of the crude extracts and of compounds **6**, **9**, **7**, and **1** were prepared in DMSO. A 2 mM solution of the chromogenic substrate MeOSuc-Ala-Ala-Pro-Val-pNA was prepared in assay buffer containing 10% DMSO. The final concentration of DMSO was 1.5%, and the final concentration of MeOSuc-Ala-Ala-Pro-Val-pNA was 100 μM. Assays were performed with a final HLE concentration of 50 ng mL^{-1}, which corresponded to an initial rate of 0.7 μM min^{-1}. To a cuvette containing 890 μL of assay buffer were added 10 μL of an inhibitor solution and 50 μL of the substrate solution, and the resulting solution was thoroughly mixed. The reaction was initiated by adding 50 μL of the HLE solution and was followed over 10 min. IC_{50} values were calculated from the linear steady-state turnover of the substrate. To determine the HLE inhibition by the crude extracts, four different inhibitor concentrations were used in duplicate experiments. The activities of trypsin and chymotrypsin were assayed with the chromogenic substrates Suc-Ala-Ala-Pro-Arg-pNA and Suc-Ala-Ala-Pro-Phe-pNA, respectively.

Acknowledgment. This work was financially supported by the DFG (SFB 624 to J.P. and M.E., GRK 804 to J.P. and M.G., and PI 430/4−1 to J.P.). We thank Profs. Bradley S. Moore and Ron Quinn for support to obtain *Streptomyces* sp. JP95, Prof. J. Salas for the kind gift of *S. albus*, Dr. M. Lalk for NMR measurements, and Stephanie Hautmann and Dr. Lixin Wei for technical assistance.

Supporting Information Available: A figure showing HPLC chromatograms of bacterial extracts, tables giving results of MS/MS analyses and primers used for gene inactivation, and detailed information concerning the computational methods used. This material is available free of charge via the Internet at http://pubs.acs.org.

JA807827K